

Afgar Ali, Sattarzadeh Bardsiri Mahla\*, Vahidi Reza\* and Farsinejad Alireza

# Predicting the possible effect of miR-203a-3p and miR-29a-3p on *DNMT3B* and *GAS7* genes expression

<https://doi.org/10.1515/jib-2021-0016>

Received July 5, 2021; accepted October 28, 2021; published online December 16, 2021

**Abstract:** Aberrant expression of genes involved in methylation, including DNA methyltransferase 3 Beta (*DNMT3B*), can cause hypermethylation of various tumor suppressor genes. In this regard, various molecular factors such as microRNAs can play a critical role in regulating these methyltransferase enzymes and eventually downstream genes such as growth arrest specific 7 (*GAS7*). Accordingly, in the present study we aimed to predict regulatory effect of miRNAs on *DNMT3B* and *GAS7* genes expression in melanoma cell line. hsa-miR-203a-3p and hsa-miR-29a-3p were predicted and selected using bioinformatics software. The Real-time PCR technique was performed to investigate the regulatory effect of these molecules on the *DNMT3B* and *GAS7* genes expression. Expression analysis of *DNMT3B* gene in A375 cell line showed that there was a significant increase compared to control ( $p$  value = 0.0015). Analysis of hsa-miR-203a-3p and hsa-miR-29a-3p indicated the insignificant decreased expression in melanoma cell line compared to control ( $p$  value < 0.05). Compared to control, the expression of *GAS7* gene in melanoma cells showed a significant decrease ( $p$  value = 0.0323). Finally, our findings showed that the decreased expression of hsa-miR-203a-3p and hsa-miR-29a-3p can hypothesize that their aberrant expression caused *DNMT3B* dysfunction, possible methylation of the *GAS7* gene, and ultimately decreased its expression. However, complementary studies are necessary to definite comment.

**Keywords:** bioinformatics; *DNMT3B* gene; *GAS7* gene; melanoma; microRNAs.

## 1 Introduction

Skin cancer that is known as the most common form of human cancer, divided into three main types: basal cell carcinoma, squamous cell carcinoma, and melanoma. Melanoma is a malignant tumor of melanocytes (special cells that produce melanin pigments) that despite its low prevalence (5%), has the highest mortality compared to other types (75%). On the other hand, the high-rate invasion of melanoma to other tissues is a considerable factor for early diagnosis and treatment of this disease. Several factors such as exposure to

---

\***Corresponding authors: Sattarzadeh Bardsiri Mahla**, Student Research Committee, Faculty of Allied Medicine, Kerman University of Medical Sciences, Kerman, Iran; Department of Hematology and Medical Laboratory Sciences, Faculty of Allied Medicine, Kerman University of Medical Sciences, Kerman, Iran; and Cell Therapy and Regenerative Medicine Comprehensive Center, Kerman University of Medical Sciences, Kerman, Iran, E-mail: [sabasatarzadeh3261@gmail.com](mailto:sabasatarzadeh3261@gmail.com); and **Vahidi Reza**, Research Center for Hydatid Disease in Iran, Kerman University of Medical Sciences, Kerman, Iran, E-mail: [reza.vahidi2009@gmail.com](mailto:reza.vahidi2009@gmail.com)  
**Afgar Ali**, Research Center for Hydatid Disease in Iran, Kerman University of Medical Sciences, Kerman, Iran  
**Farsinejad Alireza**, Department of Hematology and Medical Laboratory Sciences, Faculty of Allied Medicine, Kerman University of Medical Sciences, Kerman, Iran; and Cell Therapy and Regenerative Medicine Comprehensive Center, Kerman University of Medical Sciences, Kerman, Iran

ultraviolet light (through DNA mutations), severe sunburn, immunodeficiency, and genetic predisposition make people more susceptible to melanoma [1–4].

Researches show that about 5–10% of melanoma cases are people who have genetic alterations or mutation in several genes including *CDKN2A* (Cyclin Dependent Kinase Inhibitor 2A), *CDK4* (Cyclin-dependent kinase 4), *BAP1* (BRCA1 associated protein-1), *POT1* (Protection Of Telomeres 1), *ACD* (Adrenocortical dysplasia), *TERF2IP* (Telomeric repeat-binding factor 2-interacting protein 1), and *TERT* (Telomerase reverse transcriptase) that lead to the tumorigenesis [5]. Recently, it is suggested that in addition to genetic alterations, changes in epigenetic pattern (abnormal promoter methylation, histone modifications, and dysexpression of small non-coding RNAs) also play a critical role in tumor formation [6, 7]. In mammals, methylation occurs mainly in CpG islands that are located in promoter, untranslated, and exonic regions of genes and through DNA methyltransferases (*DNMT1*, *DNMT3A* and *DNMT3B*). Recent studies indicate that abnormal methylation (increase or decrease) of CpG islands may result in tumorigenesis, so that increased methylation in the regulatory regions of tumor suppressor and DNA repair genes silences them and leads to cancer progression [8]. Abnormal DNA methylation is considered as an important epigenetic marker in melanoma pathogenesis [9] and dysexpression of methyltransferases such as *DNMT3B*, can alter methylation pattern in genes promoter [10, 11]. One of the important regulators of *DNMT3B* are small non-coding molecules called microRNAs, that are able to bind to the UTR regions of the target genes (through their "seed" region with 2–8 nucleotides) and act as post-transcriptional modification regulators. Evidences have shown that microRNA expression patterns for each cancer can be different and therefore used as a clinical prognostic factor [12, 13]. Dysregulation of these molecules can alter the expression pattern of DNA methyltransferases such as *DNMT3B* and lead to abnormal methylation process. There are many genes that their expression affected by improper methylation pattern; for example, growth arrest-specific genes (*GAS* gene family) that organize several biological functions including microfilament organization, neuronal differentiation, apoptosis, and cell cycle regulation. *GAS7* which is located at 17P13.1, mainly expressed in differentiated brain cells and cerebellar purkinje neurons and its product i.e., *GAS7* protein, plays an important role in nervous system development. In addition, this gene also has tumor suppressor activity [14, 15]. According to this information, dysfunction of microRNAs can play an important role in the development of cancer, such as melanoma [12]. Therefore, in the present study, we aimed to predict microRNAs involved in *DNMT3B* gene methylation through bioinformatics approaches and examined their effect on *DNMT3B* and *GAS7* genes expression in melanoma cells.

## 2 Materials and methods

### 2.1 MicroRNA and target mRNA prediction

Because of overexpression of *DNMT3B* gene in many tumor cells, it was selected and subsequently analyzed using DianamT, miRanda, miRDB, miRWalk, RNAhybrid, PICTAR4, PICTAR5, PITA, RNA22, and Targetscan through the miRWalk 2.0 database hyperlink (<http://zmf.umm.uni-heidelberg.de/apps/zmf/mirwalk/predictedmirnagene.html>). According to the algorithm of the mentioned programs, a large number of miRNAs were predicted based on the following criteria: the longest seed region, conserved pairing of seed region, and the number of software that simultaneously predicted the target miRNAs. Finally, two microRNAs were selected based on the mentioned items for the *DNMT3B* gene binding.

### 2.2 Stem-loop, primers, and special probes design

The sequences of predicted microRNAs were retrieved from the microRNA database (<http://www.mirbase.org/>). These target microRNAs included hsa-miR-203a-3p and hsa-miR-29a-3p. In order to detection of the minimum amount of target microRNAs and increase the necessary sensitivity, we used the stem loop sequence from Faridi et al. publication [16]. The designed miRNA could detect the last six nucleotides at the end of stem-loop which complement the 3' region of the each mature miRNA (Figure 1). To design forward primers, almost all mature microRNAs sequences were used. Then, the melting temperature ( $T_m$ ) of the primers and probes and also secondary structure of all sequences was adjusted using Gene Runner software and mFold web server (<http://mfold.rna.albany.edu/?q=mfold/>) (<https://bio.tools/mfold>). To determine the specificity of each primer, the blast

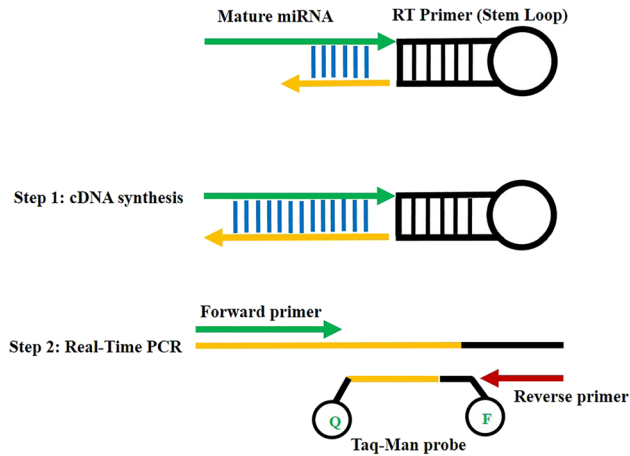


**Figure 1:** Schematic representation of stem loop structure and miRNAs amplification using the stem loop RT approach. This method consists of two steps: 1 – stem loop RT amplification (cDNA synthesis) 2 – real-time PCR reaction. In this method, first six nucleotides of 3' of miRNA target are reversed, complemented, and attached to 3' position of stem loop RT and cDNA is synthesized by reverse transcriptase. The synthesized product (cDNA) is then amplified by real-time PCR and universal TaqMan probe.

**Table 1:** Designed RT stem-loops, primers and probe.

| miRNA                 | Accession number | Designed sequence                                             |
|-----------------------|------------------|---------------------------------------------------------------|
| RT primer miR-203a-3p | MIMAT0031890     | GTATGCTGCTACCTCGGACCCTGCTTAGTGCCATGCCTGCCATCGAGCAGCATAACACTGT |
| RT primer miR-29a-3p  | MIMAT0004503     | GTATGCTGCTACCTCGGACCCTGCTTAGTGCCATGCCTGCCATCGAGCAGCATACTGAAC  |
| RT primer U6          | NR_004394.1      | GTATGCTGCTACCTCGGACCCTGCTTAGTGCCATGCCTGCCATCGAGCAGCATACTGAAT  |
| F-miR-203a-3p         | MIMAT0031890     | AGTGGTTCTTAACAGTTCAACAGTT                                     |
| F-miR-29a-3p          | MIMAT0004503     | GCGTGATTTCTTTGGTGTTCAG                                        |
| F-U6                  | NR_004394.1      | GCAAGGATGACACGCAAATTCG                                        |

Taq man probe sequence: FAM 5'AGTGCCATGCCTGCCATCGAGC 3' BHQ-1, universal reverse primer sequence: GCTGCTACCTCGGACCCT, F: forward primer.

primer analysis was performed using the Primer-Blast (<https://www.ncbi.nlm.nih.gov/tools/primer-blast>). Then, the experimental specificity of each microRNA was examined and confirmed by amplification sequence analysis (Real-time PCR). The sequences of designed reverse transcriptase (RT) stem-loops, primers and probe are presented in Table 1.

### 2.3 Cell preparation

A375 melanoma cell line (ATCC<sup>®</sup> CRL-1619<sup>™</sup>) and normal melanocytes (ATCC<sup>®</sup> PCS-200-013<sup>™</sup>) were purchased from the cell bank of Pasteur Institute of Iran (IPI), Tehran, Iran. The cells were cultured in Dulbecco's minimum Eagle's medium (DMEM) with 10% FBS, 2 mM glutathione, 100 U/mL of penicillin and 100 µg/mL of streptomycin. Transfer to fresh media was performed when confluency was around 90% and finally, cells were harvested using 0.25% trypsin-EDTA.

### 2.4 Experimental design

In relation to experimental design, gene expression was performed by real-time PCR with three biological and two technical replicates. In this case, three separate samples were prepared from each cell line and then RNA extraction and cDNA synthesis were performed for each sample. Finally, the gene expression in each sample was evaluated using real-time PCR and in duplicate.

### 2.5 Extraction of target microRNAs and RNAs

Extraction of target microRNAs was carried out with a slight modification of the RNA extraction protocol of "Sinaclone RNX-Plus Solution for total RNA isolation". Briefly, 1 mL of RNX- Plus extraction solution was added to  $5-6 \times 10^6$  cells. The cells were incubated for 3 min, then 200 µL of 1-bromo-3-chloropropane solution added to each tube and centrifuged at 4 °C (12,000g for 25 min). The supernatant was separated and transferred to a new sterile tube and the previous step was repeated with 100 µL of 1-bromo-3-chloropropane. Finally, the aqueous phase was transferred to another tube and the equal volume of isopropanol was added. The tubes were kept overnight at -20 °C (20 min for total RNA) and then centrifuged at 4 °C (12,000g for 1 h). After centrifugation, the supernatant was discarded and 1 mL of 70% ethanol was added and centrifuged at 12,000g for 30 min. The

supernatant was discarded again and tubes were kept upside down at room temperature. At the end, 50  $\mu\text{L}$  of DEPC-Treated Water and 5 units of RNase free-DNase I enzyme were added to each tube, incubated for 10 min at room temperature, and then inactivated for 5 min at 80  $^{\circ}\text{C}$ . The concentration and purity of the extracted miRNAs and total RNA were determined and finally, all samples were stored at  $-70^{\circ}\text{C}$  until analysis.

## 2.6 cDNA synthesis and real-time PCR

Following RNA extraction, 1000 ng of each sample was reversed using Mu-MLV reverse transcriptase according to the Thermo Scientific™ RevertAid RT Reverse Transcription Kit protocol. The cDNA was stored at  $-70^{\circ}\text{C}$  until analysis. The qPCR reaction was performed on a mixture of 12.5  $\mu\text{L}$  of SYBR™ Green PCR Master Mix, 0.1  $\mu\text{M}$  of probe, 0.2  $\mu\text{M}$  of each oligonucleotide primers and 2  $\mu\text{L}$  of cDNA. Real-time PCR reaction occurred under these conditions: initial denaturation at 95  $^{\circ}\text{C}$  for 40s, followed by 45 cycles consist of denaturation at 95  $^{\circ}\text{C}$  for 40s, annealing at 60  $^{\circ}\text{C}$  for 20s, and final expansion at 72  $^{\circ}\text{C}$  for 35s. The  $\beta$ -actin gene was used as the internal reference gene. Finally, PCR efficiency and expression of each mRNA were assessed using linreg software (LinRegPCR (11.0) – Gene Quantification). A  $p$  value  $< 0.05$  was considered statistically significant.

## 2.7 MicroRNA cDNA synthesis and real-time PCR

Following miRNA extraction, cDNA was synthesized using Mu-MLV reverse transcriptase. Four  $\mu\text{L}$  of extracted miRNA (adjusted for 2000 ng miRNA) was added to 1.5  $\mu\text{L}$  of stem-loop (1.100 dilution of 100  $\mu\text{M}$  stock) and 5  $\mu\text{L}$  of double distilled water. This mixture was incubated for 5 min at 65  $^{\circ}\text{C}$  in a thermocycler. Immediately, 2  $\mu\text{L}$  of dNTP (10 mM), 4  $\mu\text{L}$  of 4 $\times$  buffer, and 0.5  $\mu\text{L}$  of RNase inhibitor (20 units), 2  $\mu\text{L}$  of DTT (10 mM), and 1  $\mu\text{L}$  of reverse transcription enzyme (50  $\mu\text{L}$ ) were added to this mixture. Synthesis of cDNA was performed for 1 h at 44  $^{\circ}\text{C}$  and 5 min at 85  $^{\circ}\text{C}$  for enzyme inactivation. The synthesized cDNA was stored at  $-20^{\circ}\text{C}$  until Real-time analysis. Real-time PCR was performed using specific forward primer and probe for each microRNA. The final mixture was consisting of 6.25  $\mu\text{L}$  of 2 $\times$  qPCR Master Mix, 0.7  $\mu\text{M}$  of reverse primer, 0.5  $\mu\text{M}$  of forward primer and 0.2  $\mu\text{M}$  of specific probe in a total volume of 12.5  $\mu\text{L}$ . The enzyme was initially activated at 95  $^{\circ}\text{C}$  for 30s, followed by 45 cycles consist of 95  $^{\circ}\text{C}$  for 15s and 60  $^{\circ}\text{C}$  for 45s. The U6 gene was selected as the internal reference gene. Statistical analysis was carried out for the relative expression of each microRNA using Pfaffl method in GraphPad Prism 9.1.2 software. A  $p$  value  $< 0.05$  was considered statistically significant.

# 3 Results

## 3.1 Predicting of miRNAs and target mRNAs, and designing of stem-loops, primers, and probes

Gene repression pathways were analyzed using various popular algorithms including miRanda, miRDB, miR-Walk, RNAhybrid, PICTAR4, PICTAR5, PITA, RNA22, and Targetscan to predict the miRNAs targets including 3' UTR region of *DNMT3B* mRNA. More than 20 miRNAs targeting *DNMT3B* gene were identified and confirmed by six miRNA prediction algorithms. As mentioned in the Materials and Methods, three criteria were applied for selection of miRNAs; the longest seed region, conserved pairing of seed region, and the number of software that simultaneously predicted the target miRNAs. According to these criteria, 2 miRNAs were selected for future study (Figure 2, Tables 2 and 3).

Specific stem-loop RT for each miRNA was designed by adding six complementary nucleotides to the 3' UTR ends of the *DNMT3B* gene. Forward primers were designed alongside the reverse primer and the TaqMan probe for qPCR. NCBI Primer-BLAST for characterization of each miRNA showed that no sequence except corresponding miRNA binds to the target sequence. Characterization results showed 100% specificity for each miRNA.

## 3.2 Expression analysis of the predicted miRNAs, *DNMT3B*, and *GAS7*:

In the A375 melanoma cell line, two miRNAs (hsa-miR-203a-3p and hsa-miR-29a-3p) were selected from several microRNAs predicted by different software algorithms. As illustrated in Figure 3a, the expression of two selected microRNAs was decreased, insignificantly ( $p < 0.05$ ). On the other hand, the *DNMT3B* gene was significantly upregulated in melanoma cells compared to control cells ( $p = 0.0015$ , Figure 3b). Compared

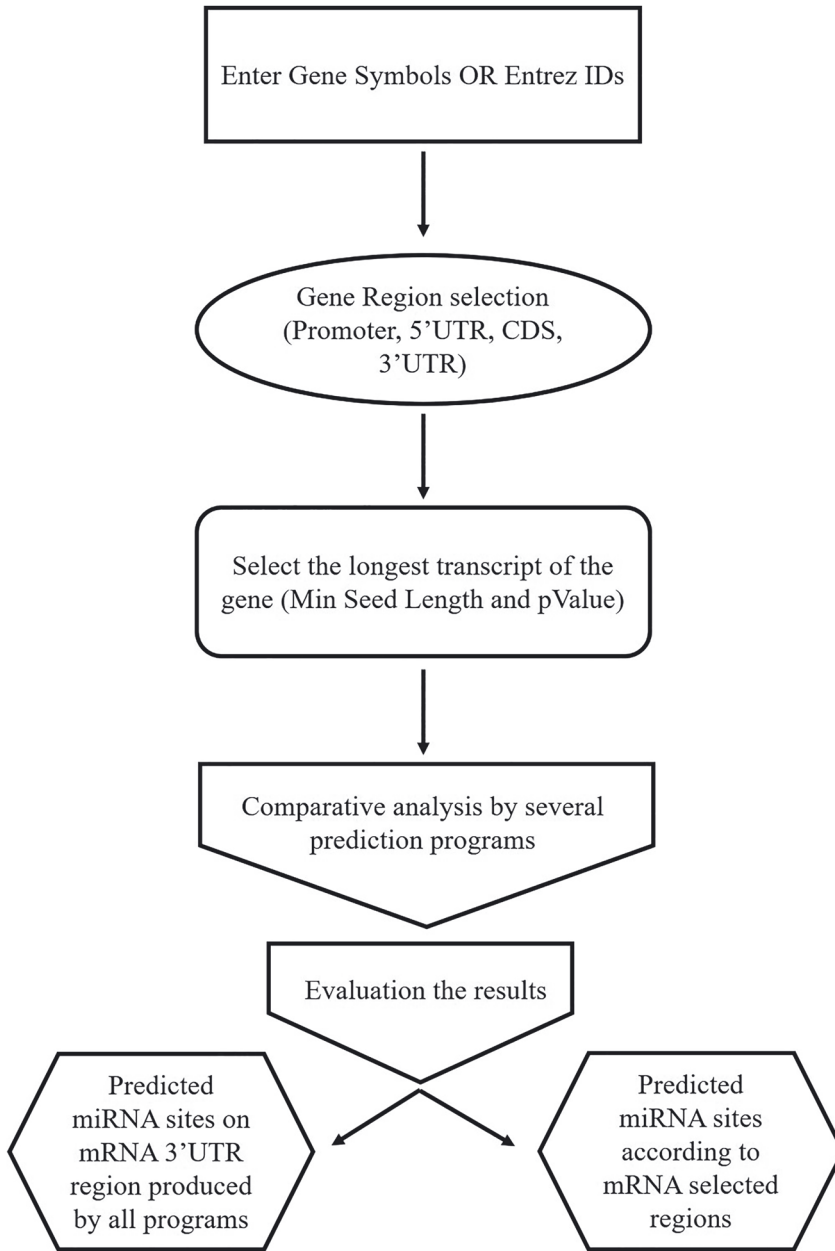


**Figure 2:** An illustration of the workflow that was performed in this study using mirwalk software. Also, this workflow was carried out for the majority of the software mentioned in this study, but with a few changes.

**Table 2:** Prediction of target miRNAs based on the number of algorithms.

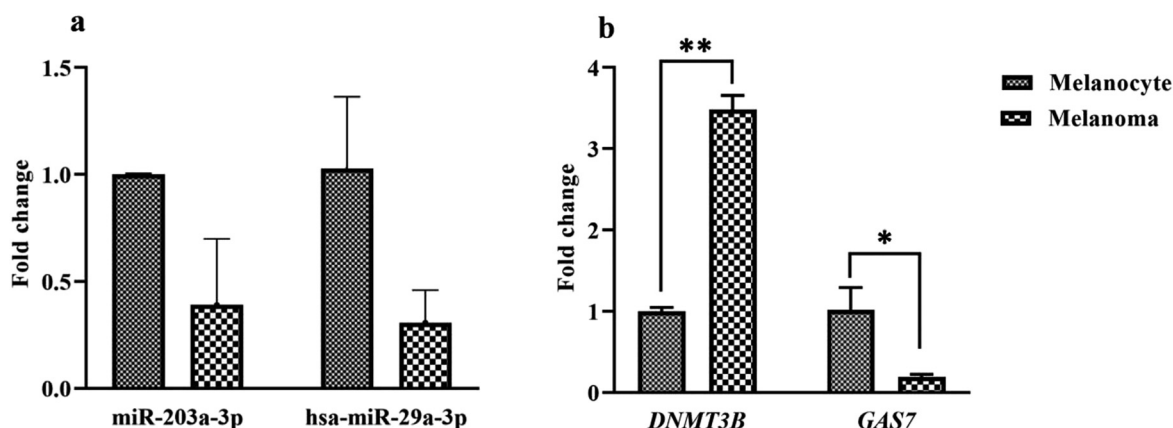
| Gene name | MicroRNA        | D | miRa | miRD | miRW | RNAh | PIC4 | PIC5 | P | R22 | Ts | Sum |
|-----------|-----------------|---|------|------|------|------|------|------|---|-----|----|-----|
| DNMT3B    | hsa-miR-203a-3p | 1 | 1    | 0    | 1    | 1    | 0    | 1    | 0 | 0   | 1  | 6   |
|           | hsa-miR-29a-3p  | 1 | 1    | 1    | 1    | 1    | 0    | 0    | 0 | 0   | 1  | 6   |

D: DIANAmt, miRa: miRanda, miRD: miRDB, miRW: miRWalk, RNAh: RNAhybrid, PIC4: PICTAR4, PIC5: PICTAR5, P: PITA, R22: RNA22, Ts: target scan.

to normal cells, the expression analysis evidenced that *GAS7* gene was significantly downregulated in the A375 cells ( $p = 0.0323$ , Figure 3b). These findings raise the possibility of methylation of *GAS7* gene following overexpression of *DNMT3B* gene.

**Table 3:** Prediction of target miRNAs based on seed length and gene region.

| Gene name     | RefSeq ID | MicroRNA        | Seed length | 3'UTR length | Region |
|---------------|-----------|-----------------|-------------|--------------|--------|
| <i>DNMT3B</i> | NM_006892 | hsa-miR-29a-3p  | 8           | 1470         | 3'UTR  |
|               | NM_006892 | hsa-miR-203a-3p | 7           | 1470         | 3'UTR  |

**Figure 3:** The expression of hsa-miR-203a-3p, hsa-miR-29a-3p, and target genes (*DNMT3B* and *GAS7*) in melanocyte and melanoma cells. As illustrated, unlike miRNAs, the expression of target genes were significantly changed in melanoma cells; *DNMT3B* was up- and *GAS7* was down-regulated, respectively. \* $p < 0.05$  and \*\* $p < 0.01$ .

## 8 Discussion

Epigenetic changes such as aberrant hypermethylation, by inducing post-transcriptional gene silencing, may contribute to inactivation of tumor suppressor genes and cancer pathogenesis [17–19]. One of the proposed mechanisms for aberrant methylation in promoters of tumor suppressor genes is the improper regulation and expression of *DNMT* genes [20]. Among all *DNMTs*, *DNMT3B* plays a major pro-tumorigenic role in human melanoma [11]. In several studies, it has been shown that there is a significant relation between aberrant expression of tumor suppressors and increased expression of *DNMT3B* gene [21, 22].

One of the important regulators of *DNMT3B* is small non-coding molecules called microRNAs [12]. Computational methods play an important role in predicting and finding miRNA targets with several designed algorithms [23]. Among these methods, high-throughput techniques such as next-generation sequencing and microarray have a high ability for determining expression profile/quantification of a large number of miRNAs. These methods are costly and not easily accessible [24]. On the other hand, the short length of some sequences such as miRNA also limits these methods [25]. As an alternative, in this study, we used bioinformatics prediction to find miRNAs that are involved in the regulation of *DNMT3B* and *GAS7* genes of melanoma cells and melanocytes. In the following, we performed stem-loop technique [26], which is highly accurate and cost-effective method (due to use of universal oligonucleotides), to investigate the expression of the predicted microRNAs (hsa-miR-203a-3p and hsa-miR-29a-3p) in melanoma cells.

Regarding miRNAs prediction, it should be noted that the ability of software is different based on the defined algorithms. For example, according to the results obtained from the used prediction software for hsa miR-29a-3p, RNA22 and PICTAR4 software were not able to detect this miRNA. On the other hand, PITA software, essentially detects microRNAs by the amount of access to sites within the target mRNA. It first evaluates the 3'UTR of important target positions, through searching the pairs of near-perfect connections, and then calculates G for each position (G is actually a score for the probability of a target site reacting with

miRNA). Considering upstream and downstream target positions for G is optional. Nevertheless, this software could not succeed in prediction hsa miR-29a-3p.

On the other hand, the miRwalk algorithm detects the sequence between miRNA and the target gene sequence, based on the longest sequences. According to the Watson-Creek complement pair base, the work of the software begins with searching in the complete gene sequence as well as the mitochondrial genome and then finding a region with at least seven matched nucleotides with the target microRNA. Next, the longest seed sequences that situated at four protein-coding regions (promoter, 5'UTR, CDS, and 3'UTR) are identified. Using different algorithmic approaches helped us to identify and predict the best miRNAs for future evaluations. The findings exhibited that hsa-miR-203a-3p and hsa-miR-29a-3p are bioinformatically able to bind to the 3'UTR region of the *DNMT3B* gene and play a possible role in its regulation. To investigate the possible indirect effect of miRNAs on expression of *DNMT3B* and *GAS7* genes, we quantified the expression of these genes in melanoma cells and normal melanocytes. The results demonstrated that the *DNMT3B* and *GAS7* genes were significantly up- and down-regulated in melanoma cells compared to melanocytes, respectively (Figure 3b). Decreased expression of *GAS7* gene in melanoma cells can be attributed to increased expression of genes involved in methylation (*DNMT3B*). Interestingly, Ashktorab et al. in a study on colorectal neoplasia showed that there were 13 significant methylated genes in 355 CpG islands (14 islands were in promoter regions). Among the most methylated genes were *ATXN7L1*, *BMP3*, *EID3*, *GPR75*, and especially *GAS7* [27, 28].

Although not significant, it seems that a 0.390-fold reduction in expression of miR-203a-3p and a 0.307-fold reduction in miR-29a-3p expression (Figure 3a) could have direct and indirect regulatory effects on *DNMT3B* and *GAS7* genes, respectively. The potential regulatory effect of miRNAs on hypermethylation of tumor suppressor genes has been confirmed in other studies [29, 30]. On the other hand, Micevic and colleagues evidenced that induction of miR-29a-3p in acute myeloid leukemia and Burkitt's lymphoma could suppress *DNMT3B* and subsequently cause promoter hypomethylation of tumor suppressor genes [11].

Overall, our findings suggest that epigenetic matters, particularly methylation, have a significant effect on tumorigenesis and should be considered as one of the vital issues in melanoma. It should be noted that this claim is based only on bioinformatics and gene expression findings; therefore, its final confirmation requires further epigenetic studies such as methylation and acetylation. Also, the expression of gene can be influenced by several miRNAs and each miRNA also may be targeted several genes [31, 32]. Therefore, in order to make a definite comment about the pathogenesis of melanoma and also factors involved in the insignificant reduction of the studied miRNAs expression, it is necessary to conduct more extensive studies on the other genes, miRNAs, and epigenetic processes such as acetylation.

In conclusion, it seems that our predicted miRNAs have a regulatory role on *DNMT3B* and *GAS7* genes and alteration of their expression can be considered as a new therapeutic approach (alone or in combination with other methods) for melanoma.

**Author contribution:** AA and RV proposed the original concept and designed the experiment and supervised all aspects of the work. MSB, AF, and A.A equally participated in the data acquisition and analysis. All authors contributed to writing the manuscript. MSB, RV, and AA provided critical reviews in order to promote the manuscript. The authors read and approved the final manuscript.

**Research funding:** This study gained the supporting grant of Student Research Committee, Faculty of Allied Medicine of Kerman University of Medical Sciences (grant No. 98001163).

**Conflict of interest statement:** The authors declare no conflict of interest.

## References

1. Das P, Deshmukh N, Badore N, Ghulaxe C, Patel P. A review article on melanoma. *J Pharmaceut Sci Res* 2016;8:112.
2. Rastrelli M, Tropea S, Rossi CR, Alaibac M. Melanoma: epidemiology, risk factors, pathogenesis, diagnosis and classification. *In Vivo* 2014;28:1005–11.

3. Gandini S, Sera F, Cattaruzza MS, Pasquini P, Picconi O, Boyle P, et al. Meta-analysis of risk factors for cutaneous melanoma: II. Sun exposure. *Eur J Cancer* 2005;41:45–60.
4. Potrony M, Badenas C, Aguilera P, Puig-Butille JA, Carrera C, Malveyh J, et al. Update in genetic susceptibility in melanoma. *Ann Transl Med* 2015;3:1–12.
5. Read J, Wadt KA, Hayward NK. Melanoma genetics. *J Med Genet* 2016;53:1–4.
6. Conway K, Edmiston SN, May R, Kuan PF, Chu H, Bryant C, et al. DNA methylation profiling in the Carolina Breast Cancer Study defines cancer subclasses differing in clinicopathologic characteristics and survival. *Breast Cancer Res* 2014;16:1–8.
7. Eccleston A, DeWitt N, Gunter C, Marte B, Nath D. Epigenetics. *Nature* 2007;447:395–6.
8. Yoo CB, Jones PA. Epigenetic therapy of cancer: past, present and future. *Nat Rev Drug Discov* 2006;5:37–50.
9. Micevic G, Theodosakis N, Bosenberg M. Aberrant DNA methylation in melanoma: biomarker and therapeutic opportunities. *Clin Epigenet* 2017;9:1–5.
10. Okano M, Bell DW, Haber DA, Li E. DNA methyltransferases Dnmt3a and Dnmt3b are essential for de novo methylation and mammalian development. *Cell* 1999;99:247–57.
11. Micevic G, Muthusamy V, Damsky W, Theodosakis N, Liu X, Meeth K, et al. DNMT3b modulates melanoma growth by controlling levels of mTORC2 component RICTOR. *Cell Rep* 2016;14:2180–92.
12. Mirzaei H, Gholamin S, Shahidsales S, Sahebkar A, Jaafari MR, Mirzaei HR, et al. MicroRNAs as potential diagnostic and prognostic biomarkers in melanoma. *Eur J Cancer* 2016;53:25–32.
13. Duursma AM, Kedde M, Schrier M, Le Sage C, Agami R. miR-148 targets human DNMT3b protein coding region. *RNA* 2008;14:872–7.
14. Ebinger M, Senf L, Wachowski O, Scheurlen W. Expression of *GAS7* in childhood CNS tumors. *Pediatr Blood Cancer* 2006;46:325–8.
15. Chao CC, Hung FC, Chao JJ. Gas7 is required for mesenchymal stem cell-derived bone development. *Stem Cell Int* 2013;2013:1–6.
16. Faridi A, Afgar A, Mousavi SM, Nasibi S, Mohammadi MA, Farajli Abbasi M, et al. Intestinal expression of miR-130b, miR-410b, and miR-98a in experimental canine echinococcosis by stem-loop RT-qPCR. *Front Vertin Sci* 2020;7:507.
17. Yun J, Song SH, Park J, Kim HP, Yoon YK, Lee KH, et al. Gene silencing of EREG mediated by DNA methylation and histone modification in human gastric cancers. *Lab Invest* 2012;92:1033–44.
18. Koga Y, Pelizzola M, Cheng E, Krauthammer M, Sznol M, Ariyan S, et al. Genome-wide screen of promoter methylation identifies novel markers in melanoma. *Genome Res* 2009;19:1462–70.
19. Jones PA, Baylin SB. The epigenomics of cancer. *Cell* 2007;128:683–92.
20. Afgar A, Fard-Esfahani P, Mehrtash A, Azadmanesh K, Khodarahmi F, Ghadir M, et al. MiR-339 and especially miR-766 reactivate the expression of tumor suppressor genes in colorectal cancer cell lines through DNA methyltransferase 3B gene inhibition. *Cancer Biol Ther* 2016;17:1126–38.
21. Ying Y, Li J, Xie H, Yan H, Jin K, He L, et al. CCND1, NOP14 and DNMT3B are involved in miR-502-5p–mediated inhibition of cell migration and proliferation in bladder cancer. *Cell Prolif* 2020;53:e12751.
22. Peres R, Furuya H, Pagano I, Shimizu Y, Hokutan K, Rosser CJ. Angiogenin contributes to bladder cancer tumorigenesis by DNMT3b-mediated MMP2 activation. *Oncotarget* 2016;7:43109.
23. Doran J, Strauss WM. Bio-informatic trends for the determination of miRNA–target interactions in mammals. *DNA Cell Biol* 2007;26:353–60.
24. Chen Y, Gelfond JA, McManus LM, Shireman PK. Reproducibility of quantitative RT-PCR array in miRNA expression profiling and comparison with microarray analysis. *BMC Genom* 2009;10:1–0.
25. Castoldi M, Schmidt S, Benes V, Hentze MW, Muckenthaler MU. miChip: an array-based method for microRNA expression profiling using locked nucleic acid capture probes. *Nat Protoc* 2008;3:321–9.
26. Chen C, Ridzon DA, Broomer AJ, Zhou Z, Lee DH, Nguyen JT, et al. Real-time quantification of microRNAs by stem–loop RT–PCR. *Nucleic Acids Res* 2005;33:e179.
27. Ashktorab H, Darempouran M, Goel A, Varma S, Leavitt R, Sun X, et al. DNA methylome profiling identifies novel methylated genes in African American patients with colorectal neoplasia. *Epigenetics* 2014;9:503–12.
28. Ashktorab H, Rahi H, Wansley D, Varma S, Shokrani B, Lee E, et al. Toward a comprehensive and systematic methylome signature in colorectal cancers. *Epigenetics* 2013;8:807–15.
29. Noguchi S, Mori T, Otsuka Y, Yamada N, Yasui Y, Iwasaki J, et al. Anti-oncogenic microRNA-203 induces senescence by targeting E2F3 protein in human melanoma cells. *J Biol Chem* 2012;287:11769–77.
30. Nguyen T, Kuo C, Nicholl MB, Sim MS, Turner RR, Morton DL, et al. Downregulation of microRNA-29c is associated with hypermethylation of tumor-related genes and disease outcome in cutaneous melanoma. *Epigenetics* 2011;6:388–94.
31. Friedman RC, Farh KK, Burge CB, Bartel DP. Most mammalian mRNAs are conserved targets of microRNAs. *Genome Res* 2009;19:92–105.

32. Krek A, Grün D, Poy MN, Wolf R, Rosenberg L, Epstein EJ, et al. Combinatorial microRNA target predictions. *Nat Genet* 2005;37:495–500.

---

**Supplementary Material:** The online version of this article offers supplementary material (<https://doi.org/10.1515/jib-2021-0016>).